

# Patchy particles at a hard wall: Orientation-dependent bonding

Cite as: J. Chem. Phys. **151**, 174903 (2019); <https://doi.org/10.1063/1.5124008>

Submitted: 11 August 2019 . Accepted: 15 October 2019 . Published Online: 06 November 2019

P. I. C. Teixeira , and F. Sciortino 



View Online



Export Citation



CrossMark

## ARTICLES YOU MAY BE INTERESTED IN

[Chain stiffness bridges conventional polymer and bio-molecular phases](#)

The Journal of Chemical Physics **151**, 174901 (2019); <https://doi.org/10.1063/1.5123720>

[Assembly of clathrates from tetrahedral patchy colloids with narrow patches](#)

The Journal of Chemical Physics **151**, 094502 (2019); <https://doi.org/10.1063/1.5109382>

[Force driven transition of a globular polyelectrolyte](#)

The Journal of Chemical Physics **151**, 174902 (2019); <https://doi.org/10.1063/1.5121407>

Lock-in Amplifiers  
up to 600 MHz



Watch



# Patchy particles at a hard wall: Orientation-dependent bonding

Cite as: *J. Chem. Phys.* **151**, 174903 (2019); doi: [10.1063/1.5124008](https://doi.org/10.1063/1.5124008)

Submitted: 11 August 2019 • Accepted: 15 October 2019 •

Published Online: 6 November 2019



View Online



Export Citation



CrossMark

P. I. C. Teixeira<sup>1,a)</sup>  and F. Sciortino<sup>2</sup> 

## AFFILIATIONS

<sup>1</sup>ISEL – Instituto Superior de Engenharia de Lisboa, Instituto Politécnico de Lisboa, Rua Conselheiro Emídio Navarro 1, P-1959-007 Lisbon, Portugal and Centro de Física Teórica e Computacional, Faculdade de Ciências da Universidade de Lisboa Campo Grande, Edifício C8, P-1749-016 Lisbon, Portugal

<sup>2</sup>Dipartimento di Fisica and CNR-ISC, Università di Roma La Sapienza, Piazzale Moro 5, I-00185 Rome, Italy

<sup>a)</sup>Electronic mail: [piteixeira@fc.ul.pt](mailto:piteixeira@fc.ul.pt)

## ABSTRACT

The well-known and widely used Wertheim thermodynamic perturbation theory (TPT) of associating fluids averages over the orientational dependence of the bonding interactions. For this reason, density functional theories based on the otherwise very successful TPT have been unable to describe the structure of patchy particle fluids at hard walls, when the coupling of positional and orientational degrees of freedom becomes important at low temperatures [N. Gnan *et al.*, *J. Chem. Phys.* **137**, 084704 (2012)]. As a first attempt at remedying this, we propose to introduce into the theory an additional, nonbonding, anisotropic interparticle potential that enforces end-to-end alignment of two-patch particles. Within the simplest mean-field approximation, this additional potential does not change the thermodynamics of the bulk system and hence preserves its phase diagram but has the qualitatively correct effect on the order parameter and density profiles at a hard wall, as determined from computer simulation.

Published under license by AIP Publishing. <https://doi.org/10.1063/1.5124008>

## I. INTRODUCTION

Recently, it has become possible to fabricate very well-defined colloidal particles with dimensions in the nanometer to micrometer range by utilizing modern synthesis techniques. Spherical colloidal particles arrange themselves in the same way that atoms do into solids, liquids, or gases. However, unlike in atomic systems, we are now able to control the interactions between colloidal particles, which provides a window into structural and thermodynamic behavior.<sup>1</sup>

Of particular interest are the so-called “patchy colloids,” the surfaces of which are patterned so that they attract each other via discrete “sticky spots” of tunable number, size, and strength. More generally, models consisting of hard particles with attractive surface sites are suitable to investigate the interplay between condensation and clustering, e.g., in protein solutions or strongly dipolar fluids (though in the latter case, aggregation is driven by long-ranged forces),<sup>2</sup> and have also been extensively used to model pure or mixed chain molecules, e.g., in industrial contexts.<sup>3</sup>

Some of the collective properties of colloids with identical patches have been intensively studied by theory and simulations, and a number of results have been obtained. In particular, if the mean number  $f$  of bonding sites per particle is greater than two, then the model exhibits liquid-vapor coexistence.<sup>4</sup> As  $f$  is reduced toward two (this can be done continuously by mixing particles with different numbers of bonding sites), the critical density goes down dramatically and liquid states become possible with vanishing packing fraction: empty liquids of spherical colloids, which are still distinct from the gaslike phase of yet lower packing fraction. These are not achievable if the interparticle interactions are isotropic, although they have been found by theory and simulation of colloidal ellipsoids,<sup>5</sup> as well as observed experimentally in suspensions of plate-like clay particles,<sup>6</sup> proteins,<sup>7</sup> and DNA-made patchy particles.<sup>8,9</sup> In addition to the equilibrium phase diagram, gelation and clustering are also strongly affected by patchiness.<sup>10</sup>

A natural generalization of the model is to allow patches to be of different types, which introduces whole matrices of energy scales and patch sizes. This was first introduced by Wertheim<sup>11–14</sup>

in the context of his first-order thermodynamic perturbation theory of association (TPT1), later reformulated by Jackson, Chapman, and Gubbins.<sup>15,16</sup> The special case of two types of patches (*A* and *B*) was extensively studied using TPT1,<sup>17–21</sup> which yields results for the liquid-vapor coexistence that are in qualitative (and in some cases semiquantitative) agreement with computer simulations. More accurate extensions of TPT1 have been proposed by Kalyuzhnyi, Cummings, and co-workers,<sup>22–26</sup> and by Marshall and Chapman.<sup>27</sup>

Considerably less attention has been devoted to inhomogeneous associating fluids, in part owing to the intrinsic complexity of their treatment. These are, however, of increasing relevance in view of advances in the micro- and nanopatterning of solid substrates, which can be used for templating colloidal self-assembly.<sup>28</sup> This relevance extends to microfluidic devices; to electronic ink, in which pigments must assemble reversibly; and to the confined environment of the living cell, where short-ranged, strongly directional hydrogen bonds play a key role. Now, Wertheim's TPT1 was initially formulated as a theory of inhomogeneous systems; i.e., it allows for position-dependent densities; in earlier work, we have applied this to study the liquid-vapor interface of colloids decorated with two patches of type *A* and up to ten patches of type *B*, for which condensation is driven exclusively by the (strongly anisotropic) interpatch attractions.<sup>29,30</sup> This extended the findings of Bernardino and Telo da Gama<sup>31</sup> to the case where all three types of bond (*AA*, *BB*, and *AB*) can form.

"Hard" interfaces – as in patchy colloids at walls or in confined environments – lead to highly nonuniform structural features, which are a challenge to model theoretically. The earliest developments, by Holovko *et al.*<sup>32–34</sup> and Henderson *et al.*,<sup>35,36</sup> were along the route of merging Wertheim's TPT with the integral equation formalism. Kierlik and Rosinberg were the first to combine density functional theory (DFT) and Wertheim's TPT1 (albeit only in the limit of complete association<sup>37,38</sup>); this they then applied to hard-sphere (HS) chains in slit-like pores.<sup>39</sup> Partially associated systems were first attacked using DFT by Segura and co-workers, who generalized Wertheim's TPT1 to pure<sup>40</sup> or mixed<sup>41</sup> patchy colloids between parallel hard walls, using Tarazona's weighted density functional (WDA) prescription.<sup>42</sup> However, these authors restricted themselves to particles with only four sites and a subset of all possible site-site interactions, where the nonzero interactions all have the same strength, as proposed by Kolafa and Nezbeda.<sup>43</sup> The same system was revisited by Patrykiewicz *et al.*<sup>44</sup> and Yu and Wu,<sup>45</sup> who combined Wertheim's TPT1, respectively, with either the modified Meister-Kroll DFT<sup>46</sup> or the very accurate fundamental-measure theory (FMT) of Rosenfeld.<sup>47</sup> The performances of integral equations and DFT in describing patchy colloids with one or two sites at a hard wall have been compared by Segura *et al.*,<sup>48</sup> who found the DFT-based method to be marginally more accurate. Later, Gnan and co-workers<sup>49</sup> applied TPT1, together with either WDA or FMT, to colloids with three identical patches at a single hard wall. Both latter sets of authors found generally good agreement with simulations, which nevertheless tends to deteriorate at low temperatures, at which the patchy particles become orientationally ordered at the wall, an effect which is neglected by both theories. Later refinements of DFT have allowed for competition between inter- and intramolecular bonding<sup>50</sup> or have relaxed the single-bonding condition of TPT1.<sup>51,52</sup>

Developing a TPT-based theory of nonuniform associating fluids which accounts for orientational order is highly nontrivial. To our knowledge, this has only been accomplished for two-patch particles in a uniform external field<sup>53</sup> or confined in a one-dimensional (1D) pore.<sup>54</sup> In both cases, it was found that association was significantly enhanced: an external field will order the particles and thus reduce the entropic penalty of association, while in 1D making one bond will align the particles involved and thus render additional bonds more likely. Studies of patchy particles interacting with specific sites on a functionalized surface<sup>55,56</sup> introduced angular dependence in the particle-surface potential only (patchy particles at a patchy surface).

In this paper, we follow a different route. Our purpose is to study a patchy particle fluid at a hard wall, following Gnan *et al.*<sup>49</sup> However, unlike these authors, we consider particles with two identical patches, which do not exhibit condensation: this allows us to concentrate on the effects on structure, without distracting complications. To this end, we introduce an additional orientation-dependent pair potential that acts between the particle centers and enforces end-to-end alignment, in order to mimic patches located at the opposite ends of a particle diameter. This new potential should not be understood as something that augments the model: it is not. Our model is still hard spheres with two identical patches. Rather, this new potential, henceforth termed "effective" for want of a better word, is something that we add to the theory to – admittedly somewhat artificially and perhaps not entirely consistently – restore the orientational dependence lost when averaging over the angular dependence of the interparticle potentials in the derivation of the TPT free energy. In a more mathematical language, we are mapping our model onto a slightly different one that the theory can handle better. This approach is inspired by models of liquid crystals (LCs) comprising spherical hard cores and where the anisotropy is introduced through the long-range part of the interaction potential only. Such a potential was used to lift the degeneracy of the LC director orientation at the nematic-isotropic or nematic-vapor interfaces.<sup>57,58</sup> This effective potential is then treated in a mean-field (MF) approximation that does not change the thermodynamics of the bulk system, which will be that of two-patch particles as described by first-order TPT (TPT1). Of course, a theory thus constructed is not fully self-consistent, but as we shall see, it is able to reproduce qualitatively, and in some cases semiquantitatively, wall-induced alignment as revealed by computer simulation.

This paper is organized as follows: in Sec. II, we recapitulate Wertheim's TPT1 and introduce the effective orientation-dependent potential that mimics the angular dependence of the interpatch attractions. The corresponding contribution to the free energy (of nonuniform phases) is derived, as are the self-consistent equations for the orientational order parameters. Section III gives details of the computer simulations performed to validate our theoretical approach. Results from theory and simulation are then compared in Sec. IV. We summarize and conclude in Sec. V.

## II. THEORY

We consider a one-component fluid of  $N$  hard spheres (HSs) of diameter  $\sigma$  and volume  $v_s = (\pi/6)\sigma^3$ , each decorated with two identical patches at its poles. The interparticle pair potential is the sum of

HS repulsion between the cores and square-well attraction between the surface patches,

$$u(\mathbf{r}_i, \hat{\mathbf{r}}_j) = u_{HS}(\mathbf{r}_{ij}) + \sum_{\alpha, \beta=1}^2 V_{ij, \alpha\beta}. \quad (1)$$

The attraction between patch  $\alpha$  on particle  $i$  at position  $\mathbf{r}_i$  and patch  $\beta$  on particle  $j$  at position  $\mathbf{r}_j$  is given by the potential originally proposed by Bol,<sup>59</sup> which has subsequently become known as the Kern-Frenkel potential,<sup>60</sup>

$$V_{ij, \alpha\beta} = V^{SW}(r_{ij})G(\hat{\mathbf{r}}_{ij}, \hat{\mathbf{r}}_{i\alpha}, \hat{\mathbf{r}}_{j\beta}), \quad (2)$$

where  $V^{SW}(r)$  is a square-well potential,

$$V^{SW}(r) = \begin{cases} \infty, & \text{if } r < \sigma \\ -\epsilon, & \text{if } \sigma < r < \sigma + \delta \\ 0, & \text{otherwise,} \end{cases} \quad (3)$$

and  $G(\hat{\mathbf{r}}_{ij}, \hat{\mathbf{r}}_{i\alpha}, \hat{\mathbf{r}}_{j\beta})$  is the angle-dependent part,

$$G(\hat{\mathbf{r}}_{ij}, \hat{\mathbf{r}}_{i\alpha}, \hat{\mathbf{r}}_{j\beta}) = \begin{cases} 1 & \left\{ \begin{array}{l} \hat{\mathbf{r}}_{ij} \cdot \hat{\mathbf{r}}_{i\alpha} > \cos \theta^{max} \\ \text{and } -\hat{\mathbf{r}}_{ij} \cdot \hat{\mathbf{r}}_{j\beta} > \cos \theta^{max} \end{array} \right. \\ 0, & \text{otherwise.} \end{cases} \quad (4)$$

Here,  $\mathbf{r}_{ij} = \mathbf{r}_i - \mathbf{r}_j$  is the interparticle vector, of length  $r_{ij} = \|\mathbf{r}_i - \mathbf{r}_j\|$ ,  $\hat{\mathbf{r}}_{ij} = \mathbf{r}_{ij}/r_{ij}$  is the unit vector along the interparticle axis, and  $\hat{\mathbf{r}}_{i\alpha}$  ( $\hat{\mathbf{r}}_{j\beta}$ ) is the unit vector pointing from the center of particle  $i$  ( $j$ ) to the center of patch  $\alpha$  ( $\beta$ ) on its surface. The model is thus specified by three parameters: the interaction energy between patches  $\epsilon$ , its range  $\delta$ , and the patch opening angle  $\theta^{max}$ . Together, the range and opening angle set the volume  $v_b$  available to a bond,

$$v_b = \frac{\pi}{3} [(\sigma + \delta)^3 - \sigma^3] (1 - \cos \theta^{max})^2. \quad (5)$$

We choose the bond volume such that each patch can only interact with one other patch at a time, and we assume that the patches are located at the poles of the HS cores. Imposing these conditions allows each patch to bond to at most one other patch, thereby ensuring that the system satisfies the assumptions made in Wertheim's TPT1.<sup>11,12,15</sup>

We now introduce an effective interparticle potential that enforces end-to-end (i.e., pole-to-pole) alignment of the particles. This is introduced in the theory only, not the simulations, as it is not intended to augment or modify our model. Rather, it is meant to mimic the angular dependence of the true interpatch potential  $V_{ij, \alpha\beta}$ , Eq. (2), which is averaged over in TPT1, and thus enable the theory to describe orientational order as seen in the simulations,

$$V_{eff}(\mathbf{r}_{ij}, \omega_i, \omega_j) = v(202) + v(022) + v(222), \quad (6)$$

where  $\omega_i$  ( $\omega_j$ ) is the orientation of particle  $i$  ( $j$ ), defined as the common direction of vectors  $\hat{\mathbf{r}}_{i\alpha}$  and  $-\hat{\mathbf{r}}_{i\alpha}$  ( $\hat{\mathbf{r}}_{j\beta}$  and  $-\hat{\mathbf{r}}_{j\beta}$ ), as the patches are identical and located at the HS poles. Furthermore,

$$v(l_1 l_2 l) = \sum_{m_1, m_2, m} v(l_1 l_2 l; r_{ij}) C(l_1 l_2 l : m_1 m_2 m) \times Y_{l_1 m_1}(\omega_i) Y_{l_2 m_2}(\omega_j) Y_{lm}^*(\omega_{ij}), \quad (7)$$

where  $\omega_{ij}$  is the orientation of  $\hat{\mathbf{r}}_{ij}$ ,  $C(l_1 l_2 l : m_1 m_2 m)$  are Clebsch-Gordan coefficients, and  $Y_{lm}(\omega)$  are spherical harmonics, in the notation of Gray and Gubbins.<sup>61</sup> The restriction to  $l = 0, 2$  comes from the symmetry of particles, which are invariant under  $\omega_i \rightarrow -\omega_i$  because the two patches are identical. For reasons that will be discussed in more detail below, we choose for  $v(l_1 l_2 l; r_{ij})$  a cutoff and shifted generalized Lennard-Jones (GLJ) functional form,

$$v(l_1 l_2 l; r_{ij}) = \begin{cases} \infty & \text{if } r_{ij} < \sigma \\ \epsilon_{l_1 l_2 l} \left[ \left( \frac{\sigma}{r_{ij}} \right)^{24} - \left( \frac{\sigma}{r_{ij}} \right)^n \right] - \epsilon_{l_1 l_2 l} \left[ \left( \frac{\sigma}{r_{max}} \right)^{24} - \left( \frac{\sigma}{r_{max}} \right)^n \right] & \text{if } \sigma \leq r_{ij} < r_{max} \\ 0 & \text{if } r_{ij} \geq r_{max}, \end{cases} \quad (8)$$

which is continuous at its (strictly finite) range  $r_{max}$ . The parameters in Eq. (8) will be chosen to best fit the numerical data. Here, the exponent 24 of the repulsive terms is meant to mimic HS repulsion.

Potentials  $v(202)$  and  $v(022)$  were introduced in Ref. 57 to fix a problem with Maier-Saupe type LC models, in which the hard cores are assumed spherical and angular dependence is implemented only via the long-range part of the interaction potential: if this only couples particle orientations [i.e., if it is  $v(220)$  in the above notation], there is no preferred director alignment at the interface between nematic and isotropic liquid or vapor phases, which is unphysical.  $v(202)$  and  $v(022)$  couple the orientation of particle  $i$ ,  $\omega_i$ , and of particle  $j$ ,  $\omega_j$ , with that of the interparticle vector,  $\omega_{ij}$ . Positive (negative)  $\epsilon_{202}$  and  $\epsilon_{022}$  enforce end-to-end (side-by-side) particle configurations and thus favor parallel (perpendicular) alignment at any

interface.  $v(222)$  has a qualitatively similar effect as it couples  $\omega_{ij}$ ,  $\omega_1$ , and  $\omega_2$  simultaneously. Figure 1 shows the energies of some of these configurations.

The grand canonical potential of the model fluid described above, in contact with a planar hard wall of area  $A$  lying in the  $xy$ -plane, is given by<sup>62</sup>

$$\frac{\Omega[\rho(z), \hat{f}(z, \theta)]}{A} = \mathcal{F}[\rho(z), \hat{f}(z, \theta)] + \int dz [V_{ext}(z) - \mu] \rho(z). \quad (9)$$

Here and in what follows, we assume that there is no structure in the plane of the hard wall, and therefore, all quantities only depend on  $z$ , the coordinate measured perpendicular to the wall, and on  $\theta$ , the angle between the line connecting the two patches at the ends (“poles”) of a particle and the  $z$ -axis. However, we shall also need

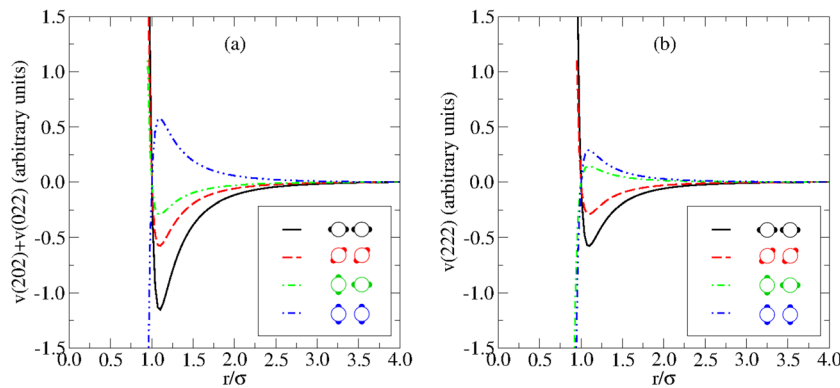


**FIG. 1.**  $r$ -dependence of (a)  $v(202) + v(022)$  and (b)  $v(222)$  potentials for some configurations of two patchy particles.

the azimuthal angle  $\phi$  in some intermediate calculations, where we denote  $\omega = (\theta, \phi)$  and  $d\omega = \sin\theta d\theta d\phi$ .

In Eq. (9),  $\rho(z)$  is the (number) density profile and  $\hat{f}(z, \theta)$  is the orientational distribution function (ODF) in the presence of the external (hard-wall) potential,

$$V_{ext}(z) = \begin{cases} 0, & \text{if } z \geq \frac{\sigma}{2} \\ +\infty, & \text{if } z < \frac{\sigma}{2}. \end{cases} \quad (10)$$

$\mu$  is the chemical potential, and  $\mathcal{F}[\rho(z), \hat{f}(z, \theta)]$  is the intrinsic Helmholtz free energy of the inhomogeneous fluid, which is independent of the external potential.  $\mathcal{F}[\rho(z), \hat{f}(z, \theta)]$  can be written as a sum of three contributions:

$$\begin{aligned} \mathcal{F}[\rho(z), \hat{f}(z, \theta)] &= \mathcal{F}_{id}[\rho(z), \hat{f}(z, \theta)] + \mathcal{F}_{hs+b}[\rho(z), X(z)] \\ &+ \mathcal{F}_{MF}[\rho(z), \hat{f}(z, \theta)], \end{aligned} \quad (11)$$

where  $X(z)$  is the spatially varying fraction of unbonded sites.

The first contribution in Eq. (11),  $\mathcal{F}_{id}$ , is the (exact) entropy of the ideal, noninteracting fluid, comprising both translational and rotational terms (as we are explicitly taking into account particle orientations),

$$\begin{aligned} \mathcal{F}_{id}[\rho(z), \hat{f}(z, \theta)] &= k_B T \int dz \rho(z) \{ \log[\Lambda^3 \rho(z)] - 1 \} \\ &+ k_B T \int dz d\omega \rho(z) \hat{f}(z, \theta) \log[4\pi \hat{f}(z, \theta)], \end{aligned} \quad (12)$$

where  $\Lambda$  is the thermal De Broglie wavelength,  $k_B$  is Boltzmann's constant, and  $T$  is the temperature.

The second contribution in Eq. (11),  $\mathcal{F}_{hs+b}$ , accounts for both excluded volume and bonding interactions. Because these have similar ranges, it was argued by Segura *et al.*<sup>40</sup> that they might be treated together within the framework of a WDA of DFT.<sup>63</sup> The idea is to write the free energy of the inhomogeneous patchy HS fluid as an integral of the free energy density of the homogeneous fluid evaluated at some effective density given by an appropriate averaging procedure. It was found that Tarazona's WDA performs better than FMT when either is combined with Wertheim's TPT1 to describe the

structure of particles with three identical patches at a hard wall.<sup>49</sup> For this reason, we shall employ the same variant of Tarazona's WDA, developed by Kim *et al.*,<sup>64</sup> and write

$$\mathcal{F}_{hs+b}[\rho(z)] = \int dz \rho(z) \Phi_{hs+b}(\bar{\rho}(z)). \quad (13)$$

The weighted density  $\bar{\rho}(z)$  is expanded as

$$\bar{\rho}(z) = \rho_0(z) + \rho_1(z) \bar{\rho}(z) + \rho_2(z) \bar{\rho}(z)^2, \quad (14)$$

with

$$\bar{\rho}(z) = \rho_0(z) + \rho_1(z) \rho_{bulk} + \rho_2(z) \rho_{bulk}^2, \quad (15)$$

where  $\rho_{bulk}$  is the bulk density and

$$\rho_i(z) = \int dz' \rho(z') w_i(|z - z'|) \quad (i = 0, 1, 2) \quad (16)$$

are convolutions of  $\rho(z)$  with appropriate weight functions,

$$w_0(z) = \frac{3}{4} (\sigma^2 - z^2) \Theta(\sigma - |z|), \quad (17)$$

$$\begin{aligned} w_1(z) &= \pi [0.0565(\sigma^4 - z^4) - 0.432(\sigma^3 - z^3) + 0.475(\sigma^2 - z^2) \\ &- 0.03317] \Theta(\sigma - |z|) + \pi [-0.0935(16\sigma^4 - z^4) \\ &+ 0.5093(8\sigma^3 - z^3) - 0.924(4\sigma^2 - z^2) + 0.576(2\sigma - |z|)] \\ &\times [\Theta(2\sigma - |z|) - \Theta(\sigma - |z|)], \end{aligned} \quad (18)$$

$$w_2(z) = \frac{5\pi^2}{144} \left[ \frac{5}{2} (\sigma^4 - z^4) - 8(\sigma^3 - z^3) + 6(\sigma^2 - z^2) \right] \Theta(\sigma - |z|), \quad (19)$$

with  $\Theta(x)$  the Heaviside step function. In Eq. (13),  $\Phi_{hs+b}$  is the excess free energy per particle of a uniform fluid of HSS with two identical patches, which in turn comprises excluded volume and bonding terms,

$$\Phi_{hs+b}(\rho) = \Phi_{hs}(\rho) + \Phi_b(\rho), \quad (20)$$

for which we use, respectively, the Carnahan-Starling approximation<sup>65</sup> and Wertheim's TPT1, as shown in the following.<sup>15</sup>

$$\Phi_{hs}(\rho) = \beta^{-1} \frac{\xi(4-3\xi)}{(1-\xi)^2}, \quad (21)$$

$$\Phi_b(\rho) = \beta^{-1}(2 \log X + 1 - X), \quad (22)$$

where  $\xi = (\pi/6)\rho\sigma^3$  is the packing fraction and  $\beta = 1/k_B T$ . The fraction of unbonded sites  $X$  is given by the law of mass action, which in this particularly simple case can be solved analytically to yield

$$X = \frac{-1 + \sqrt{1 + 4\xi\Delta}}{2\xi\Delta}, \quad (23)$$

with  $\Delta$  the bond partition function,

$$\Delta = \frac{1}{v_s} \int_{v_b} g_{ref}(\mathbf{r}) [\exp(\beta\epsilon) - 1] d\mathbf{r}. \quad (24)$$

The integral in Eq. (24) is calculated over  $v_b$ , the volume of a bond,  $g_{ref}(\mathbf{r})$  is the pair correlation function (PCF) of the reference (HS) system, and  $v_s$  is the volume of a HS. As in an earlier work, we employ a linear approximation for the PCF,<sup>66</sup> with the result

$$\Delta = \frac{v_b}{v_s} [\exp(\beta\epsilon) - 1] \frac{1 - C_1\xi - C_2\xi^2}{(1-\xi)^3}, \quad (25)$$

where

$$C_1 = \frac{1}{2} \left[ -8 - \frac{27}{4} \left(1 + \frac{\delta}{\sigma}\right)^4 - 1 \right], \quad (26)$$

$$C_2 = -\frac{9}{2} \left[ 1 - \frac{3}{4} \left(1 + \frac{\delta}{\sigma}\right)^4 - 1 \right]. \quad (27)$$

Finally, the third contribution in Eq. (11),  $\mathcal{F}_{MF}$ , is that of the orientation-dependent effective potential, Eq. (6), which we write, in the usual mean-field (MF) approximation,<sup>57</sup> as (see the Appendix for details of derivation)

$$\begin{aligned} \mathcal{F}_{MF}[\rho(z), \eta(z)] &= \frac{1}{2} \int dz_i dz_j \rho(z_i) [\bar{v}(202; |z_i - z_j|) \eta(z_i) \\ &\quad + \bar{v}(022; |z_i - z_j|) \eta(z_j)] \rho(z_j) \\ &\quad + \frac{1}{2} \int dz_i dz_j \rho(z_i) \eta(z_j) \bar{v}(322; |z_i - z_j|) \\ &\quad \times \rho(z_j) \eta(z_j), \end{aligned} \quad (28)$$

where  $\bar{v}(022; z)$  are given in the Appendix, and we have defined the orientational order parameter as

$$\eta(z) = \int P_2(\cos \theta) \hat{f}(z, \theta) d\omega, \quad (29)$$

with  $P_2(x) = \frac{1}{2}(3x^2 - 1)$  the second Legendre polynomial.  $\eta(z)$  is thus a measure of particle orientations. Positive (negative) values of  $\eta(z)$  indicate preferentially perpendicular (parallel) alignment to the hard wall at a given  $z$ .

In deriving Eq. (28), we have used the fact that the system is (by reasonable assumption) axially symmetric with respect to  $z$  and dropped any terms containing the azimuthal angle  $\phi$ , which would vanish on integration. Besides its simplicity and qualitative

correctness, the MF approximation has the key advantage that Eq. (28) vanishes in isotropic bulk phases.<sup>61</sup> This implies that at the MF level, the thermodynamics of the present model is exactly the same as that of HS with two attractive patches. In particular, there is no liquid-vapor critical point, which allows us to concentrate on the structural effects of patchiness.

Once we are in possession of the Helmholtz free energy, Eq. (11), the grand canonical potential, Eq. (9), can be minimized with respect to the density profile  $\rho(z)$  and the ODF  $\hat{f}(z, \theta)$  to obtain the Euler-Lagrange (EL) equations for the system,

$$\frac{\delta\Omega[\rho(z), \hat{f}(z, \theta)]}{\delta\rho(z)} = 0 \Leftrightarrow \frac{\delta F[\rho(z), \hat{f}(z, \theta)]}{\delta\rho(z)} = \mu - V_{ext}(z), \quad (30)$$

$$\frac{\delta\Omega[\rho(z), \hat{f}(z, \theta)]}{\delta\hat{f}(z, \theta)} = \lambda, \quad (31)$$

where  $\lambda$  is a Lagrange multiplier that enforces normalization of the ODF. This yields the following pair of nonlinear integral equations that can only be solved numerically,

$$\bar{\rho}(z) = \rho_{bulk} \exp\{\beta\mu_{exc} - \beta V_{ext}(z) + c^{(1)}[z; \rho(z)]\}, \quad (32)$$

$$\hat{f}(z, \theta) = Z^{-1} \exp\{-\beta[a(z) + b(z)]P_2(\cos \theta)\}, \quad (33)$$

with  $\mu_{exc}$  the excess chemical potential, and

$$\begin{aligned} c^{(1)}[z; \rho(z)] &= -\beta\Phi_{hs+b}(\bar{\rho}(z)) - \beta \int dz' \rho(z') \frac{\partial\Phi_{hs+b}(\bar{\rho}(z))}{\partial\bar{\rho}(z)} \frac{\delta\bar{\rho}(z')}{\delta\rho(z)} \\ &\quad - \beta \log \frac{4\pi}{Z} - \beta b(z) \left[ \frac{\epsilon_{202}}{\epsilon_{222}} + \eta(z) \right], \end{aligned} \quad (34)$$

$$\begin{aligned} \frac{\delta\bar{\rho}(z')}{\delta\rho(z)} &= w(z - z', \bar{\rho}(z')) + w(z - z', \rho_{bulk}) \\ &\quad \times \int dz'' \rho(z'') \frac{\partial w'(z' - z'', \bar{\rho}(z''))}{\partial\bar{\rho}(z'')}, \end{aligned} \quad (35)$$

$$a(z) = \int dz' \bar{v}(202; |z - z'|) \rho(z'), \quad (36)$$

$$b(z) = \int dz' \bar{v}(222; |z - z'|) \rho(z') \eta(z'), \quad (37)$$

$$Z = \int d\omega \exp\{-\beta[a(z) + b(z)]P_2(\cos \theta_i)\}. \quad (38)$$

Readers are referred to Refs. 49 and 57 for details of their derivation.

The surface tension can be calculated as the excess grand canonical potential per unit area,

$$\gamma = \frac{\Omega[\rho(z), \hat{f}(z, \omega)] - \Omega_{bulk}}{A} = \frac{\Omega[\rho(z), \hat{f}(z, \omega)] + pV}{A}, \quad (39)$$

where  $\Omega_{bulk} = -pV$  is the grand canonical potential of the uniform fluid at the coexistence pressure  $p$  and chemical potential  $\mu$  ( $V$  is the volume of the system).

### III. SIMULATIONS

We have studied a system composed of  $N = 10\,800$  particles enclosed in a cubic box of edge length  $30\sigma$  ( $\rho\sigma^3 = 0.4$ ), with standard periodic boundary conditions along directions  $x$  and  $y$ , in the  $NVT$  ensemble, via the standard Monte Carlo (MC) method. Two hard walls constrain the  $z$  coordinates of all particles to be always between  $\pm 15\sigma$ . The elementary rototranslational moves consist of a random translation of at most  $\pm 0.05\sigma$  and a random rotation of at most  $\pm 0.1$  rad. We have investigated a range of temperatures extending from  $k_B T/\epsilon = 0.30$  down to  $k_B T/\epsilon = 0.08$ . For all these temperatures, there were no difficulties in equilibrating the sample. The number of MC steps (each step being defined as  $N$  attempts to move a particle) increased progressively from  $10^6$  to  $10^7$  on lowering the temperature.

### IV. RESULTS

Equation (32) was solved iteratively by a variant of the Picard method, in which the density profile at the  $(j + 1)$ th step,  $\rho^{(j+1)}(z)$ , is taken to be a linear combination of  $\rho^{(j)}(z)$  and  $\tilde{\rho}^{(j)}(z)$  using a mixing parameter  $\alpha$ ,<sup>67</sup>

$$\rho^{(j+1)}(z) = (1 - \alpha)\rho^{(j)}(z) + \alpha\tilde{\rho}^{(j)}(z). \quad (40)$$

Iteration was started from a uniform density  $\rho^{(0)}(z) = \rho_{bulk}$ . At each step,  $\eta(z)$  was computed using Eqs. (29), (33), and (38), and the (nonequilibrium) surface tension using Eq. (39). The calculation was deemed to have converged when

$$\int dz \left[ \rho^{(j+1)}(z) - \rho^{(j)}(z) \right]^2 < 10^{-8}, \quad (41)$$

$$\int dz \left[ \eta^{(j+1)}(z) - \eta^{(j)}(z) \right]^2 < 10^{-8}, \quad (42)$$

$$\frac{|\gamma^{(j+1)} - \gamma^{(j)}|}{\gamma^{(j)}} < 10^{-4}, \quad (43)$$

which in most cases was achieved in fewer than 100 steps for  $\alpha = 0.1$ .

Comparison between theory and simulation requires finding optimal values for the parameters entering  $V_{eff}(\mathbf{r}_{ij}, \omega_i, \omega_j)$ , i.e.,  $\epsilon_{222}$ ,  $\epsilon_{202}$ ,  $\epsilon_{022}$ ,  $n$ , and  $r_{max}$ . Because all particles (and patches) are identical,  $\epsilon_{202} = \epsilon_{022}$ , which reduces the number of fit parameters by one. Interestingly, we were able to obtain fairly good agreement between theory and simulation over an interval of temperatures by keeping  $\epsilon_{222}$ ,  $\epsilon_{202} = \epsilon_{022}$ , and  $n$  fixed, and varying just  $r_{max}$ , the range of the effective orientation-dependent potential  $V_{eff}(\mathbf{r}_{ij}, \omega_i, \omega_j)$ . Table I collects all potential parameters used. Though we do not rule out that comparable success may be achieved with functional forms other than a GLJ, cutting off the potential at a finite range turned out to be crucial: if  $r_{max} \rightarrow \infty$ , then  $\eta(z)$  will not decay to zero away from the wall, in contradiction with simulations.

Figure 2 shows the density profiles [panels (a), (c), (e), and (g), left column] and order parameter profiles [panels (b), (d), (f), and (h), right column] at bulk density  $\rho_{bulk}\sigma^3 = 0.4$  and five reduced temperatures  $T^* = k_B T/\epsilon$ . At the highest temperatures considered ( $T^* = 0.30$  and  $0.20$ ), MC simulations yield fairly high densities right at

TABLE I. Parameters of the (short-ranged) interpatch interaction and of the effective orientation-dependent potential used in this work.

$\cos \theta^{max}$	$\delta/\sigma$	$\epsilon_{202}/\epsilon = \epsilon_{022}/\epsilon$	$\epsilon_{222}/\epsilon$	$n$
0.895	0.119	0.6	0.6	4

the wall [ $\rho(z \sim 0.5\sigma) \gg \rho_{bulk}$ ] and a moderate amount of layering up to  $z \sim 2\sigma$  [see Fig. 2(a)], similar to those exhibited by a HS fluid at a hard wall, which is the infinite-temperature limit of our model. These features are remarkably well reproduced by theory. As already reported in Ref. 49, particles align with their axes parallel to the wall, leading to  $\eta(z) < 0$  for  $0 < z \lesssim 1.5\sigma$ . This effect is weak at  $T^* = 0.30$  and  $0.20$ , for which theory and simulation agree very well [see Fig. 2(b)]. At these temperatures, there is little association (see Fig. 3), so we have mostly individual particles lying flat against the wall to expose both their patches and thus maximize the number of bonds they can form. Notice that theory is able to reproduce not only the dip in  $\eta(z)$  at  $z \sim \sigma$  but also the blip at  $z \sim 1.5\sigma$ , which is indicative of (very weak) alignment perpendicular to the wall. This likely arises from a second layer of particles partially penetrating the gaps in the first layer and bonding with particles in the first layer that are not parallel to the wall.

Lowering the temperature drives much stronger wall-induced orientational order [ $\eta(z \sim \sigma)$  becomes more negative; see Figs. 2(d) and 2(f)]: longer chains form, which like all elongated hard objects tend to align parallel to a hard wall<sup>68</sup> while at the same time – because they are very open aggregates – decreasing the density there [see Figs. 2(c) and 2(e)]. One additional factor contributing to desorption is that additional bonds can be more easily formed if particles move away from the wall.

At the lowest reduced temperature shown [ $T^* = 0.11$ ; see Figs. 2(g) and 2(h)], agreement between theory and simulation deteriorates considerably, with theory overestimating both amplitudes and positions of the maxima and minima of  $\eta(z)$ . This may be a consequence of the MF approximation overestimating the contribution of the effective orientation-dependent potential to the free energy (recall that MF is essentially a high-temperature approximation). At yet lower temperatures ( $T^* < 0.11$ ), no meaningful fit could be accomplished, even if the potential strengths  $\epsilon_{l_1 l_2 l}$  and exponent  $n$  were also used as fit parameters.

In Fig. 3, we plot  $X(z)$ , the fraction of unbonded sites, from simulation and theory. Theory predicts that bonding is always more extensive at the wall than in bulk, and more so as  $T^*$  is lowered. This is what one would expect from bulk Wertheim TPT, given that the density from theory is also higher at the wall than in the bulk [see Figs. 2(a), 2(c), 2(e), and 2(g)]. Simulation, however, finds  $\rho(z = 0.5\sigma) < \rho_{bulk}$  for  $T^* \leq 0.20$  and less bonding at the wall than in bulk for all temperatures investigated. As the WDA of DFT is known to provide a very accurate description of the HS-hard wall interface, this discrepancy probably means that our effective orientation-dependent potential approach is not able to capture the full richness of bond directionality.

In an attempt to rationalize the above results, we computed the mean sizes of aggregates (which in this case are linear chains), from simulation and Wertheim's theory. These are compared with the

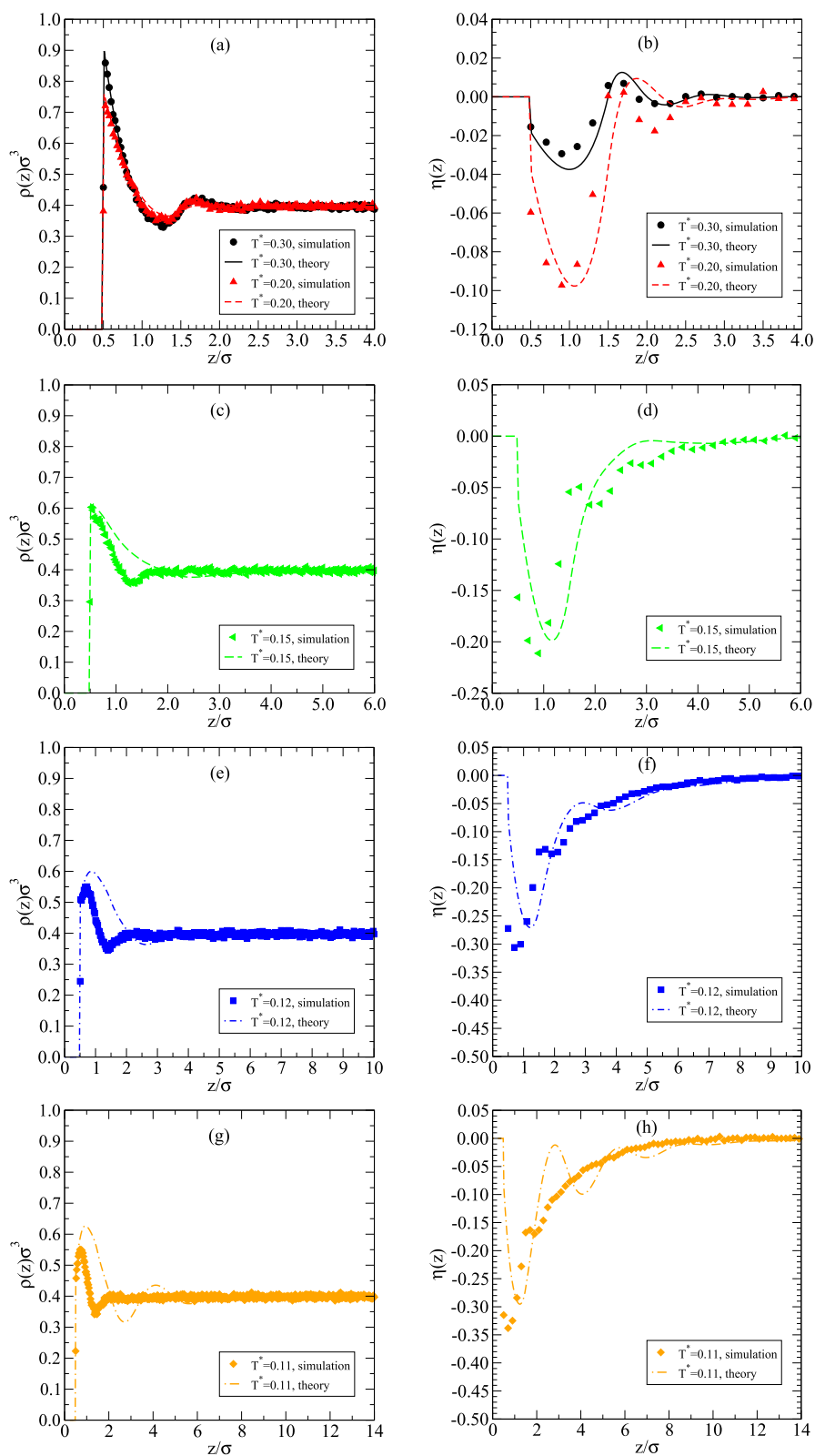


**FIG. 2.** Density profiles (left column) and order parameter profiles (right column) from MC simulation (symbols) and theory (lines) of patchy particles at a hard wall, for  $\rho_{bulk}\sigma^3 = 0.4$ : (a) and (b)  $T^* = 0.30$  and  $T^* = 0.20$ ; (c) and (d)  $T^* = 0.15$ ; (e) and (f)  $T^* = 0.12$ ; and (g) and (h)  $T^* = 0.11$ . The parameters used to compute the theoretical curves are listed in Table I and Fig. 4.

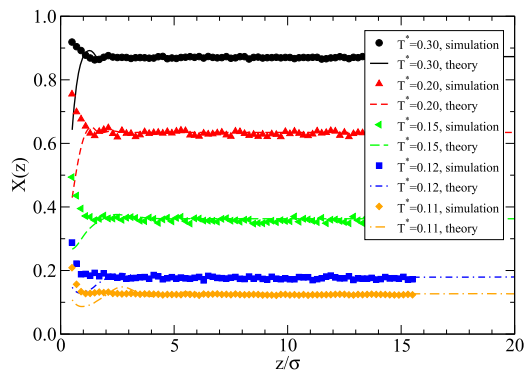


**FIG. 3.** Fraction of unbonded patches profiles for bulk density  $\rho_{\text{bulk}}\sigma^3 = 0.4$  and reduced temperatures as given.

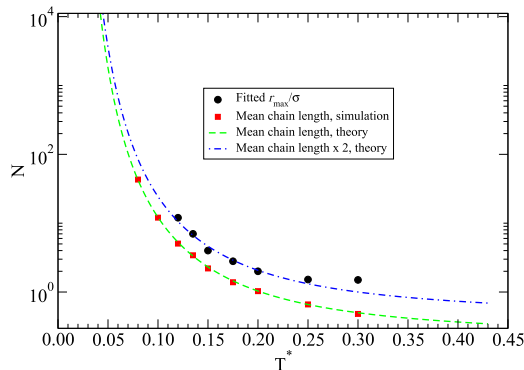


**FIG. 4.** Comparison of range  $r_{\text{max}}$  of effective anisotropic potential used to fit the density and order parameter MC data of Fig. 2 with mean size of aggregates (i.e., chain lengths) in units of number of particles, from both Wertheim's theory and MC simulation.

fitted  $r_{\text{max}}$  in Fig. 4. Interestingly, for most temperatures, there appears to be a clear correlation, with  $r_{\text{max}}$  being approximately two times the mean chain length in units of  $\sigma$ . It thus appears that the directional character of the interpatch interaction manifests itself through an increase in its range as the temperature is lowered, suggesting that  $V_{\text{eff}}(\mathbf{r}_{ij}, \omega_i, \omega_j)$  has to correlate particle orientations over distances of the order of the average chain length.

## V. DISCUSSION AND CONCLUSIONS

We have attempted to remedy a well-known, but difficult to fix, shortcoming of DFT implementations of the Wertheim TPT of associating fluids by introducing an effective, orientation-dependent potential that mimics the directional character of the short-ranged bonding interactions, which is averaged over in TPT. This was treated at the MF level and combined with the WDA approximation of DFT, which consists in writing the free energy of the inhomogeneous patchy particle fluid as an integral of its TPT1 free energy density, evaluated at an appropriate weighted density.

For particles with two identical patches at their poles in contact with a hard wall, the theory is able to reproduce the qualitative features of layering and of the preferential alignment of particles parallel to the wall seen in the simulations, over a reasonably wide interval of temperatures, with just one temperature-dependent fit parameter:  $r_{\text{max}}$ , the range of the effective orientation-dependent potential. We have also found a consistent correlation between  $r_{\text{max}}$  and the mean size of aggregates (linear chains). The theory is, however, unable to predict the smaller degree of bonding close to the wall, which appears to be a shortcoming of our approach.

The angular dependence of the effective potential is dictated by the patch positions on the particle surface, so, in principle, other patch configurations could be modeled in this way, albeit at a cost of added analytical complexity. One additional constraint is that the effective potential must not change the patchy fluid thermodynamics.

## ACKNOWLEDGMENTS

P.I.C.T. acknowledges financial support from the Fundação para a Ciência e Tecnologia (Portugal) through Contract No. UID/FIS/00618/2019. F.S. acknowledges support from MIUR-PRIN Grant No. 2017Z55KCW.

## APPENDIX: EFFECTIVE ORIENTATION-DEPENDENT POTENTIAL CONTRIBUTION TO THE FREE ENERGY

The MF expression for the contribution of long-range interactions to the Helmholtz free energy of an inhomogeneous fluid reads<sup>62</sup>

$$\mathcal{F}_{\text{MF}}[\rho(\mathbf{r}), \hat{f}(\mathbf{r}, \omega)] = \frac{1}{2} \int d\mathbf{r}_i d\omega_i d\mathbf{r}_j d\omega_j \rho(\mathbf{r}_i, \omega_i) \times V_{\text{eff}}(\mathbf{r}_i, \omega_i; \mathbf{r}_j, \omega_j) \rho(\mathbf{r}_j, \omega_j), \quad (\text{A1})$$

where  $\rho(\mathbf{r}, \omega)$  is the density-orientation profile in the presence of some external potential,  $\mathbf{r} = (x, y, z)$  is the set of position coordinates, and  $\omega = (\phi, \theta, \chi)$  is the set of orientation coordinates (Euler angles) of a particle. The density profile and ODF thus follow:

$$\rho(\mathbf{r}) = \int d\omega \rho(\mathbf{r}, \omega), \quad (\text{A2})$$

$$\hat{f}(\mathbf{r}, \omega) = \frac{\rho(\mathbf{r}, \omega)}{\rho(\mathbf{r})}. \quad (\text{A3})$$

In the case of a planar, featureless wall lying in the  $xy$ -plane, the system is nonuniform in the  $z$ -direction only, about which it is also reasonable to assume axial symmetry, i.e.,  $\rho(\mathbf{r}) \equiv \rho(z)$  and  $\hat{f}(\mathbf{r}, \omega) \equiv \hat{f}(z, \theta)$ . Using Eqs. (A2) and (A3), Eq. (A1) becomes

$$\mathcal{F}_{\text{MF}}[\rho(z), \hat{f}(z, \theta)] = \frac{1}{2} \int dz_i d\omega_i dz_j d\omega_j \rho(z_i) \hat{f}(z_i, \theta_i) \times \overline{V_{\text{eff}}}(|z_i - z_j|, \theta_i, \theta_j) \rho(z_j) \hat{f}(z_j, \theta_j), \quad (\text{A4})$$

where we have defined the laterally averaged effective potential  $\overline{V_{\text{eff}}}(z_{ij}, \theta_i, \theta_j)$  by integrating over  $x_{ij}$  and  $y_{ij}$  (in practice, the integration is performed using cylindrical coordinates, for symmetry reasons),

$$\begin{aligned} \overline{V}_{\text{eff}}(z_{ij}, \theta_i, \theta_j) &= \int dx_{ij} dy_{ij} [v(202; r_{ij})P_2(\cos \theta_i) + v(022; r_{ij})P_2(\cos \theta_j) + v(222; r_{ij})P_2(\cos \theta_i)P_2(\cos \theta_j)]P_2(\cos \theta_{ij}) \\ &= \int_0^{2\pi} d\phi_{ij} \int_0^{+\infty} R_{ij} dR_{ij} [v(202; R_{ij}, z_{ij})P_2(\cos \theta_i) + v(022; R_{ij}, z_{ij})P_2(\cos \theta_j) \\ &\quad + v(222; R_{ij}, z_{ij})P_2(\cos \theta_i)P_2(\cos \theta_j)] \times \frac{1}{2} \left( \frac{3z_{ij}^2}{R_{ij}^2 + z_{ij}^2} - 1 \right) \\ &= \overline{v}(202; z_{ij})P_2(\cos \theta_i) + \overline{v}(022; z_{ij})P_2(\cos \theta_j) + \overline{v}(222; z_{ij})P_2(\cos \theta_i)P_2(\cos \theta_j), \end{aligned} \quad (\text{A5})$$

where

$$\overline{v}(l_1 l_2 l; z_{ij}) = \begin{cases} -\epsilon_{l_1 l_2 l} \left\{ [(6n^2 - 12n)\pi\sigma^n \log \sigma + (n^2 - 2n)\pi r_{\text{max}}^n \left(\frac{\sigma}{r_{\text{max}}}\right)^n + [(12n - 6n^2)\pi \log r_{\text{max}} + (-n^2 - 4n + 12)\pi]\sigma^n + (6n - 12)\pi r_{\text{max}}^n z_{ij}^2 + (2n - n^2)\pi r_{\text{max}}^n \sigma^2 \left(\frac{\sigma}{r_{\text{max}}}\right)^n + n^2 \pi r_{\text{max}}^2 \sigma^n - 2n\pi r_{\text{max}}^n \sigma^2] \times [(2n^2 - 4n)r_{\text{max}}^n]^{-1} \right\} & \text{if } z_{ij} < \sigma \\ -\epsilon_{l_1 l_2 l} \left\{ (6n^2 - 12n)\pi r_{\text{max}}^n \left(\frac{\sigma}{r_{\text{max}}}\right)^n z_{ij}^{m+2} \log z_{ij} + z_{ij}^n \left\{ [(12 - 6n)\pi\sigma^n + (2n - n^2)\pi r_{\text{max}}^n \left(\frac{\sigma}{r_{\text{max}}}\right)^n + (12n - 6n^2)\pi\sigma^n \log r_{\text{max}}] z_{ij}^2 + 2n\pi r_{\text{max}}^2 \sigma^n + (n^2 - 2n)\pi r_{\text{max}}^{n+2} \left(\frac{\sigma}{r_{\text{max}}}\right)^n \right\} + (4n - 12)\pi r_{\text{max}}^n \sigma^n z_{ij}^2 \right\} & \text{if } \sigma < z_{ij} < r_{\text{max}} \\ 0 & \text{if } z_{ij} > r_{\text{max}}. \end{cases} \quad (\text{A6})$$

Substitution of Eq. (A5) into Eq. (A4) then gives Eq. (28).

## REFERENCES

- A. van Blaaderen, *Nature* **439**, 545 (2006).
- P. I. C. Teixeira, J. M. Tavares, and M. M. Telo da Gama, *J. Phys.: Condens. Matter* **12**, R411–R434 (2000).
- W. G. Chapman, K. E. Gubbins, G. Jackson, and M. Radosz, *Fluid Phase Equilib.* **52**, 31–38 (1989).
- E. Bianchi, J. Largo, P. Tartaglia, E. Zaccarelli, and F. Sciortino, *Phys. Rev. Lett.* **97**, 168301 (2006).
- S. Varga, E. Meneses-Júarez, and G. Odriozola, *J. Chem. Phys.* **140**, 134905 (2014).
- B. Ruzicka, E. Zaccarelli, L. Zulian, R. Angelini, M. Sztucki, A. Moussad, T. Narayanan, and F. Sciortino, *Nat. Mater.* **10**, 56–60 (2011).
- A. Boire, P. Menut, M. H. Morel, and C. Sanchez, *Soft Matter* **9**, 11417–11426 (2013).
- S. Biffi, R. Cerbino, F. Bomboi, E. M. Paraboschi, R. Asselta, F. Sciortino, and T. Bellini, *Proc. Natl. Acad. Sci. U. S. A.* **110**, 15633 (2013).
- F. Bomboi, S. Biffi, R. Cerbino, T. Bellini, F. Bordini, and F. Sciortino, *Eur. Phys. J. E* **38**, 64 (2015).
- F. Sciortino, *Eur. Phys. J. B* **64**, 505–509 (2008).
- M. S. Wertheim, *J. Stat. Phys.* **35**, 19–34 (1984).
- M. S. Wertheim, *J. Stat. Phys.* **35**, 35–47 (1984).
- M. S. Wertheim, *J. Stat. Phys.* **42**, 459–476 (1986).
- M. S. Wertheim, *J. Stat. Phys.* **42**, 477–492 (1986).
- G. Jackson, W. G. Chapman, and K. E. Gubbins, *Mol. Phys.* **65**, 1–31 (1988).
- W. G. Chapman, G. Jackson, and K. E. Gubbins, *Mol. Phys.* **65**, 1057–1079 (1988).
- J. M. Tavares, P. I. C. Teixeira, and M. M. Telo da Gama, *Mol. Phys.* **107**, 453–466 (2009).
- J. M. Tavares, P. I. C. Teixeira, and M. M. Telo da Gama, *Phys. Rev. E* **80**, 021506 (2009).
- J. Russo, J. M. Tavares, P. I. C. Teixeira, M. M. Telo da Gama, and F. Sciortino, *Phys. Rev. Lett.* **106**, 085703 (2011).
- J. Russo, J. M. Tavares, P. I. C. Teixeira, M. M. Telo da Gama, and F. Sciortino, *J. Chem. Phys.* **135**, 034501 (2011).
- J. M. Tavares and P. I. C. Teixeira, *J. Phys.: Condens. Matter* **24**, 284108 (2012).
- Y. V. Kalyuzhnyi, H. Docherty, and P. T. Cummings, *J. Chem. Phys.* **133**, 044502 (2010).
- Y. V. Kalyuzhnyi, H. Docherty, and P. T. Cummings, *J. Chem. Phys.* **135**, 014501 (2011).
- Y. V. Kalyuzhnyi, S. P. Hlushak, and P. T. Cummings, *J. Chem. Phys.* **137**, 244910 (2012).
- Y. V. Kalyuzhnyi, B. D. Marshall, W.-G. Chapman, and P. T. Cummings, *J. Chem. Phys.* **139**, 044909 (2013).
- Y. V. Kalyuzhnyi and P. T. Cummings, *J. Chem. Phys.* **139**, 104905 (2013).
- B. D. Marshall and W. G. Chapman, *J. Chem. Phys.* **139**, 214106 (2013).
- Y. D. Yin, Y. Lu, B. Gates, and Y. N. Xia, *J. Am. Chem. Soc.* **123**, 8718–8729 (2001).
- A. Oleksy and P. I. C. Teixeira, *Phys. Rev. E* **91**, 012301 (2015).
- P. I. C. Teixeira, *Colloids Surf., A* **514**, 63–68 (2017).
- N. Bernardino and M. M. Telo da Gama, *Phys. Rev. Lett.* **109**, 116103 (2012).
- M. F. Holovko and E. V. Vakarín, *Mol. Phys.* **84**, 1057–1064 (1995).
- E. V. Vakarín and M. F. Holovko, *Mol. Phys.* **90**, 63–73 (1997).
- E. Vakarín, M. F. Holovko, and Y. Duda, *Mol. Phys.* **91**, 203–214 (1997).
- D. Henderson, A. Kovalenko, O. Pizio, and S. Sokolowski, *Physica A* **231**, 254–264 (1996).
- D. Henderson, O. Pizio, S. Sokolowski, and A. Trokhymchuk, *Physica A* **244**, 147–163 (1996).

- <sup>37</sup>E. Kierlik and M. L. Rosinberg, *J. Chem. Phys.* **97**, 9222–9239 (1992).
- <sup>38</sup>E. Kierlik and M. L. Rosinberg, *J. Chem. Phys.* **99**, 3950–3965 (1993).
- <sup>39</sup>E. Kierlik and M. L. Rosinberg, *J. Chem. Phys.* **100**, 1716–1730 (1994).
- <sup>40</sup>C. J. Segura, W. G. Chapman, and K. P. Shukla, *Mol. Phys.* **90**, 759–771 (1997).
- <sup>41</sup>C. J. Segura, J. Zhang, and W. G. Chapman, *Mol. Phys.* **99**, 1–12 (2001).
- <sup>42</sup>P. Tarazona, U. M. B. Marconi, and R. Evans, *Mol. Phys.* **60**, 573–595 (1987).
- <sup>43</sup>J. Kolafa and I. Nezbeda, *Mol. Phys.* **61**, 161–175 (1987).
- <sup>44</sup>A. Patrykiewicz, S. Sokolowski, and D. Henderson, *Mol. Phys.* **95**, 211–218 (1998).
- <sup>45</sup>Y.-X. Yu and J. Wu, *J. Chem. Phys.* **116**, 7094–7103 (2002).
- <sup>46</sup>M. Calleja and G. Rickayzen, *Mol. Phys.* **79**, 809–818 (1993).
- <sup>47</sup>Y. Rosenfeld, *Phys. Rev. Lett.* **63**, 980–983 (1989).
- <sup>48</sup>C. J. Segura, E. V. Vakarín, W. G. Chapman, and M. F. Holovko, *J. Chem. Phys.* **108**, 4837–4848 (1998).
- <sup>49</sup>N. Gnan, D. de las Heras, J. M. Tavares, M. M. Telo da Gama, and F. Sciortino, *J. Chem. Phys.* **137**, 084704 (2012).
- <sup>50</sup>B. D. Marshall, A. J. García-Cuéllar, and W. G. Chapman, *J. Chem. Phys.* **136**, 154103 (2012).
- <sup>51</sup>B. D. Marshall and W. G. Chapman, *J. Chem. Phys.* **138**, 044901 (2013).
- <sup>52</sup>S. Sokolowski and Y. V. Kalyuzhnyi, *J. Phys. Chem. B* **118**, 9076–9084 (2014).
- <sup>53</sup>B. D. Marshall, W. G. Chapman, and M. M. Telo da Gama, *Phys. Rev. E* **88**, 060301(R) (2013).
- <sup>54</sup>B. D. Marshall, *J. Chem. Phys.* **142**, 234906 (2015).
- <sup>55</sup>S. Tripathi and W. G. Chapman, *J. Chem. Phys.* **119**, 12611–12620 (2003).
- <sup>56</sup>A. Haghmoradi, L. Wang, and W. G. Chapman, *J. Phys.: Condens. Matter* **29**, 044402 (2017).
- <sup>57</sup>J. H. Thurtell, M. M. Telo da Gama, and K. E. Gubbins, *Mol. Phys.* **54**, 321–332 (1985).
- <sup>58</sup>B. Tjijto-Margo, A. K. Sen, L. Mederos, and D. E. Sullivan, *Mol. Phys.* **67**, 601–614 (1989).
- <sup>59</sup>W. Bol, *Mol. Phys.* **45**, 605–616 (1982).
- <sup>60</sup>N. Kern and D. Frenkel, *J. Chem. Phys.* **118**, 9882–9889 (2003).
- <sup>61</sup>C. G. Gray and K. E. Gubbins, *Theory of Molecular Fluids* (Clarendon Press, Oxford, 1984), Vol. 1.
- <sup>62</sup>R. Evans, *Adv. Phys.* **28**, 143–200 (1979).
- <sup>63</sup>Also note that within TPT1, the bonding interaction has no angular dependence (it is averaged over orientations), so  $\mathcal{F}_{hs+b}$  is a functional of  $\rho(z)$  only.
- <sup>64</sup>S. Kim, M. Calleja, and G. Rickayzen, *J. Phys.: Condens. Matter* **7**, 8053–8063 (1995).
- <sup>65</sup>N. F. Carnahan and K. E. Starling, *J. Chem. Phys.* **51**, 635–636 (1969).
- <sup>66</sup>I. Nezbeda and G. Iglesias-Silva, *Mol. Phys.* **69**, 767–774 (1990).
- <sup>67</sup>R. Roth, *J. Phys.: Condens. Matter* **22**, 063102 (2010).
- <sup>68</sup>A. Poniewierski, *Phys. Rev. E* **47**, 3396–3403 (1993).